Civil Engineering and Architecture 12(3A): 2159-2180, 2024 http://www.hrpub.org
DOI: 10.13189/cea.2024.121317

# Analysis of Condensation Risk in A Wall Section in the Context of Climate Change Scenarios

**Pelin Saricioglu[1,*], İdil Aycam[2], Gulsu Ulukavak Harputlugil[3]**

[1]Graduate School of Natural and Applied Sciences, Gazi University, Turkey
[2]Department of Architecture, Faculty of Architecture, Gazi University, Turkey
[3]Department of Architecture, Faculty of Architecture, Cankaya University, Turkey

*Received November 27, 2023; Revised February 9, 2024; Accepted March 5, 2024*

***Cite This Paper in the Following Citation Styles***

***(a):*** *[1] Pelin Saricioglu, İdil Aycam, Gulsu Ulukavak Harputlugil , "Analysis of Condensation Risk in A Wall Section in the Context of Climate Change Scenarios," Civil Engineering and Architecture, Vol. 12, No. 3A, pp. 2159 - 2180, 2024. DOI: 10.13189/cea.2024.121317.*

***(b):*** *Pelin Saricioglu, İdil Aycam, Gulsu Ulukavak Harputlugil (2024). Analysis of Condensation Risk in A Wall Section in the Context of Climate Change Scenarios. Civil Engineering and Architecture, 12(3A), 2159 - 2180. DOI: 10.13189/cea.2024.121317.*

Copyright©2024 by authors, all rights reserved. Authors agree that this article remains permanently open access under the terms of the Creative Commons Attribution License 4.0 International License

**Abstract** The effects of climate change can be seen in many areas. Although there are many causes of climate change (changes in solar radiation, differences in the Earth's orbit, continental shifts and changes in the atmosphere), one of the most noticeable causes in the 21st century is anthropogenic effects. One area where these impacts can be seen is the construction sector in buildings and building façades. Climate change will change assumptions about façade design in the coming decades. For this reason, it is important to develop climate change projections for existing and new buildings. For this purpose, the literature has three basic climate models. Therefore, the aim of this study is to compare the condensation risk for a wall section in a city with a humid-temperate climate (Zonguldak, Turkey) using HadGEM, MPI and GFDL climate models according to RCP8.5 scenario data for the historical period 2015 and the future year 2081. Within the scope of the study, the average temperatures and relative humidity values were obtained from GDM (General Directorate of Meteorology) by choosing 2081 and 2015, which are frequently used in climate change studies based on the literature. In the method, the projection results for the historical and future periods were compared and became the basis for the next stage. In the next step, based on the literature, the condensation control in the wall section was compared for the past and future using the Glaser method, which is frequently used in condensation control in wall sections and included in the TS 825 standard created for Turkey, which corresponds to EN ISO 13788 and DIN 4108 standards. According to the results, the humidity and temperature fluctuations in the future period and increase in averages are important problems that need to be addressed in detail in façade design and the impact of condensation risk. Therefore, according to the condensation control calculations made in the wall section detail, condensation risk occurs in the future period. Consequently, assumptions in façade design will need to change for existing and future buildings to accommodate condensation risk.

**Keywords** Climate Change, Glaser Method, Future Projections, Condensation Risk, Climate Change Models

## 1. Introduction

In a recent report, the UN Climate Change Secretariat notes changes in climate indicators, including temperature, precipitation, sea-level, ocean acidification and extreme weather conditions [1]. Droughts, floods, hurricanes, severe storms, heatwaves, wildfires, cold spells and landslides are among the climate risks observed [2], [3]. The first climate change scenarios were developed by the IPCC (Intergovernmental Panel on Climate Change) in 1990. Soon thereafter, an attempt was made to characterize the impacts of climate change within the framework of these scenarios. Today, the scenarios represent key drivers,

processes, impacts (physical, ecological and economic) and potential responses important for informing climate change policies. The scenarios developed consider different assumptions regarding population growth, energy use, economies, technological developments and changes in agriculture and land use [4]. Four scenarios exist based on different emission scenarios called Representative Concentration Pathways (RCPs) – RCP2.6, RCP4.5, RCP6 and RCP8.5. Of the four RCPs, RCP4.5 and RCP8.5 are the most favored scenarios globally from the IPCC's next generation scenario family. The route with the maximum radiative forcing and concentration is RCP8.5. This scenario implies higher GHG emissions compared to the other scenarios and indicates the upper limit of RCPs. Under the RCP8.5 scenario, radiative forcing is assumed to reach 8.5 W/m$^2$ and equivalent $CO_2$ concentrations around 1370 ppm in 2100 [5]. Concurring with a report by the IPCC, high temperatures have been seen in certain worldwide zones within the current decade. For example, the temperature recorded for 2015 was so high that it was acknowledged as the hottest year of the decade. Agreeing with analysts, the mean temperature of the period between 2081 and 2100 is evaluated to be 0.3-4.8ºC higher than that between 1986 and 2005 [5].

Global climate models (GCMs, also known as General Circulation Models) describe global climate statistics, such as global mean surface temperature. Researchers have used GCMs to evaluate the impact of climate change in many study disciplines [6]. As a reflection of technology development, calculations in GCMs have become easier, computational capacity has increased, adding components to the models has become easier and resolutions have reached better levels (150-200km today, while it was around 700km in the past) [7]. Regionally downscaled data obtained from GDM (General Directorate of Meteorology) and derived from HadGEM (Earth System Model of the Hadley Center of the United Kingdom Meteorological Office), GFDL (Geophysical Fluid Dynamics Laboratory) and MPI (Max Plank Institute) for GCMs are used in the study. To use GCM models in studies, it is necessary to downscale them to regional data (RCM-Regional Circulation Model). Some tools use downscaling methods for future GCM weather data, such as "CCWorldWeatherGen" or "WeatherShiftTM tool" for building simulations [8]. In addition, the data characteristics vary according to the study purpose and simulation program to be used. For example, hourly data are generally used in studies on energy performance and buildings. Since a simulation program is not used in this study and the method is based on monthly data, monthly climate data is used.

More and more engineers and architects are considering sustainability when designing buildings due to the ongoing temperature rise brought on by climate change and its potentially disastrous effects on building performance [6]. The built environment is susceptible to the detrimental effects of climate change, and among these sectors, buildings are particularly vulnerable [9]. Climate change impacts buildings in several important ways, including increased flooding and winter storms, increased summer cooling needs, greater risk of subsidence and water shortages [10]. Such consequences are categorized by Hrabovszky-Horváth et al. into four groups. The first category is structural damage caused by environmental events including landslides, storms, floods and snowfall. The second category is building construction, which includes problems with water supply and construction fixation systems. Concerns about building materials, such as diminished frost resistance, UV resistance and insulation effectiveness, fall under the third category. The final group demonstrates how higher outdoor temperatures brought on by climate change impact the internal built environment [11], [12]. According to future climate projections, temperatures will increase, cooling demands will increase while heating demands will decrease and precipitation anomalies will be seen. According to Rahif et al. [13], resistance to extreme temperatures and cooling strategies will gain importance in buildings due to increasing temperatures. Hayles et al. [14], in their study, reveal that indoor conditions will deteriorate in the summer months as a result of climate change in buildings in Wales, which is in the northern temperate climate zone. Their study for the summers of 2030 and 2070 shows the potential for lower indoor environmental quality due to increased relative humidity. Regardless of housing typology, relative humidity will increase everywhere. Baborska-Naroznya and Grudzinska [15] examined overheating in a high-rise retrofit apartment block in Leeds, northern England, and found it could be avoided if shading measures such as blinds were in place to prevent excessive solar heat gains. According to one study, although it varies according to climate zones, cooling energy demand will be highest in temperate and cold regions, and solutions such as thermal insulation and shading in the building envelope will reduce these effects, more studies are needed to determine whether these will be sufficient [12]. When the studies are examined, it can be seen that shading elements and insulation improvements of existing buildings should be made in the context of measures to be taken for building façades regarding the impact of climate change.

From the viewpoint of the façade, buildings are largely responsible for over 40% of energy consumption and 50% of air pollutant emissions due to significant heat losses through the envelope. Therefore, improving energy performance of building assemblies plays a key role in improving the whole building's energy efficiency. However, façade renovation needs a complex design that considers not only the immediate reduction of heat losses, but also specific issues such as durability, sustainability, health and comfort of users [16]. The primary instrument for assessing a building façade's performance is evaluation of the condensation risk. Condensation occurs when water

vapor in the air contacts a colder surface and turns into liquid. This can happen inside building envelopes when warm, moist air penetrates the walls or roofs and meets a cooler surface, such as a metal or concrete element. The result is moisture buildup that can lead to corrosion, wood rot, cracked tiles or masonry, and other forms of material degradation [17]. Flood-related dampness may lead to the growth of mold, bacteria and protozoa on building surfaces, which can release harmful bioaerosols into the indoor air [18]. Additionally, structural weakening can happen when moisture seeps into the building and causes concrete, steel or wood to rust or degrade. Safety risks and expensive repairs may result from this. In this regard, on-site evaluations and costly, time-consuming laboratory tests can be used to conduct hygrothermal, or heat and moisture transfer analysis of the building envelope. The Glaser approach and dynamic simulations can take the place of these two methods for the design process [16]. The Glaser method is described by the DIN 4108 and EN ISO 13788 standards to define condensation and hygrothermal performance [19], [20]. One limitation is that the Glaser method assumes steady-state conditions, which may not accurately represent the dynamic nature of climate change. The application of the Glaser method with climate change variables provides valuable insights into the condensation risk in wall sections under changing climate conditions [21]. In the literature Verlag [19] compares the Glaser method and WUFI-Pro, which is a hygrothermal analysis based simulation software, in terms of moisture content. In conclusion, Verlag [19] says that more accurate HAM simulation may be able to rule out the risk of moisture accumulation in situations when the envelope under consideration fails the Glaser method assessment. For this reason, a model of this type must also be chosen when assessing moisture condensation. In another study, Çağman and Ünver [22] used Glaser method for analyzing the 3 wall types with Kütahya, Turkey's climatic data. They put forward the effect of insulation and wall material types in context of condensation water amount with Glaser method. Langmans et al. [23] present a useful three-dimensional heat and vapour model for calculating the likelihood of interstitial condensation in building enclosures. In actuality, the model is a three-dimensional Glaser method implementation. The paper concludes with a real-world example, in which choosing a design for an energetic retrofit of a curtain wall system shows how the model can be applied. Biserni and Imbiombato [17] analyses a building's exterior wall as a means of condensation problem with Glaser method. Regarding the case study, the findings show that condensation happens in the winter and that it's possible for the moisture to evaporate entirely in the summer. Gołębiewski and Pietruszka [24] show the findings of a study on hemp-lime composite. The structure of the external walls was determined using the test results, and the Glaser method was used to analyze the risk of interstitial water vapor condensation. It was discovered that in all Polish climate zones, there was either no condensation at all or very little, in which case it did not build up in the following years.

In the literature, studies are comparing HAM (heat, air and moisture) tools and the Glaser method, and in these studies, the superiority of simulation programs in terms of analysis sensitivity has been demonstrated. As a result, analyzing mold risk in wall sections using HAM tools or the Glaser method is a different evaluation method regarding the types of data they use and the outputs they give. However, using the Glaser method, this study is limited to mold risk analysis in wall cross-section with future climate data. Future studies, as seen in the literature, aim to make and compare analyses using these methods, increase the number of climate change prediction models, and make analyses with different scenarios.

Although projections have been made for different places in the literature on climate change, the fact this study was conducted for a province in a humid-temperate climate in Turkey contributes to the literature in terms of providing comparison with climate change studies conducted on places with similar climates. In addition, as emphasized in the literature, fluctuations in climate data in the future periods and changes in peak values have been revealed with the projections. The most important emphasis in the study is that the moisture risk projections in the wall cross-section provide information to architects about the façade design, but the difference from similar studies is that it combines the moisture problems that may occur on the façades with analysis based on the literature and addresses the problems that need to be considered for the future period with a broad perspective.

### 1.1. Climate Change Projections and Effects on Building Façades

Research has been conducted all around the world to find out how climatic change affects the energy consumption patterns of buildings [25]. For example, there will be more frequent heatwaves of greater intensity and duration, and the residential sector in Qatar will use 30% more cooling energy [26]. The rise in heatwave frequency is an essential feature of climate change. Only half the residential structures have air conditioning equipment, according to a survey in 2011. These facts may illustrate the idea that these structures are not built to withstand extreme weather, just regular cold climate weather conditions [6].

In addition, not many studies exist on how climatic changes may affect building façades. Important daily weather processes that contribute to premature deterioration of the exterior of structures as climate effects include wind-driven rain (WDR), temperature fluctuations, freeze-thaw cycles, frost effects, wetting and drying of porous materials, the effects of solar and ultraviolet (UV) radiation, and chemical deposition on metals from the atmosphere [27]. WDR is one of the main sources of

moisture for building exteriors. It can apparently affect structural durability and hygrothermal performance. Currently, most of the research with WDR distribution emphasizes an isolated building rather than a combination layout. WDR distribution is influenced by many factors such as building shape, building configuration, wind direction, wind speed and rainfall intensity, which determine the complexity of related research [28]. Future climate predictions are associated with an increase in interstitial (between tissues) relative humidity, which will lead to an increase in dampness and mold. It shows, in most cases, the parts of buildings closest to the ground are most affected by deterioration, as building materials (stones, mortars, bricks) are porous and allow water to rise through capillary action [29].

Climate has a significant impact on the performance of fa çades and influences the deterioration and natural aging of exterior building components throughout their service life. Climatic factors, such as temperature, precipitation, wind and solar radiation, interact directly with fa çade claddings and trigger degradation mechanisms, resulting in defects. Cladding is more susceptible to deterioration as it is the outer layer of the fa çade system and is directly exposed to climatic loads such as temperature, solar radiation, humidity, precipitation and wind, as well as elements in the atmosphere (e.g., pollutants and living organisms). External factors affect the performance of renders and environmental actions are often the cause of defects in fa çade cladding. Exposure to high temperatures can contribute to increased rate and depth of carbonation [30].

Through dynamic thermal simulations, it was shown that adequate use of PCMs would reduce total hours of discomfort and cooling energy loads [31].

Also, most studies on the impact of climate change on corrosion are based on a dose-response function equation and do not account for seasonal variability in the region. For example, a Norwegian study Gr øntoft [32] shows that increased (decreased) precipitation in a region synchronized with increasing (decreasing) temperatures will lead to an increase (decrease) in corrosion. Moreover, climate change is expected to result in an increase in average temperature of 0.9-5.4 C depending on location by the end of this century, which suggests the degradation of plastics due to exposure to solar radiation will only increase in the future.

As shown in **Figure 1**, the predictions and detrimental consequences of climate change on structures can be summed. High temperatures, one of the climate change characteristics, will impact building air conditioning and cooling systems, as well as how these systems function and what they can do, as shown in **Figure 1**. The need for cooling will grow, and as temperatures rise, so will the energy requirements of structures. Moreover, there will be a greater demand for natural and artificial shading. A further effect of rising temperatures is a shift in indoor comfort levels, which may call for more cooling and propose using air conditioning and other alternative remedies. The additional effects of climate change, such as abnormal precipitation and elevated humidity, will have a special impact on fa çades and fa çade systems. Extreme humidity will have a negative impact on building envelope materials, causing corrosion and fungal growth, which will shorten their lifespan and reduce their durability. Similarly, severe temperatures may affect the lifespan of materials used for fa çades, such as plastic. Flood effects will specifically affect and damage buildings in coastal regions and their foundations as one of the regional or local outcomes relating to precipitation anomalies [33].

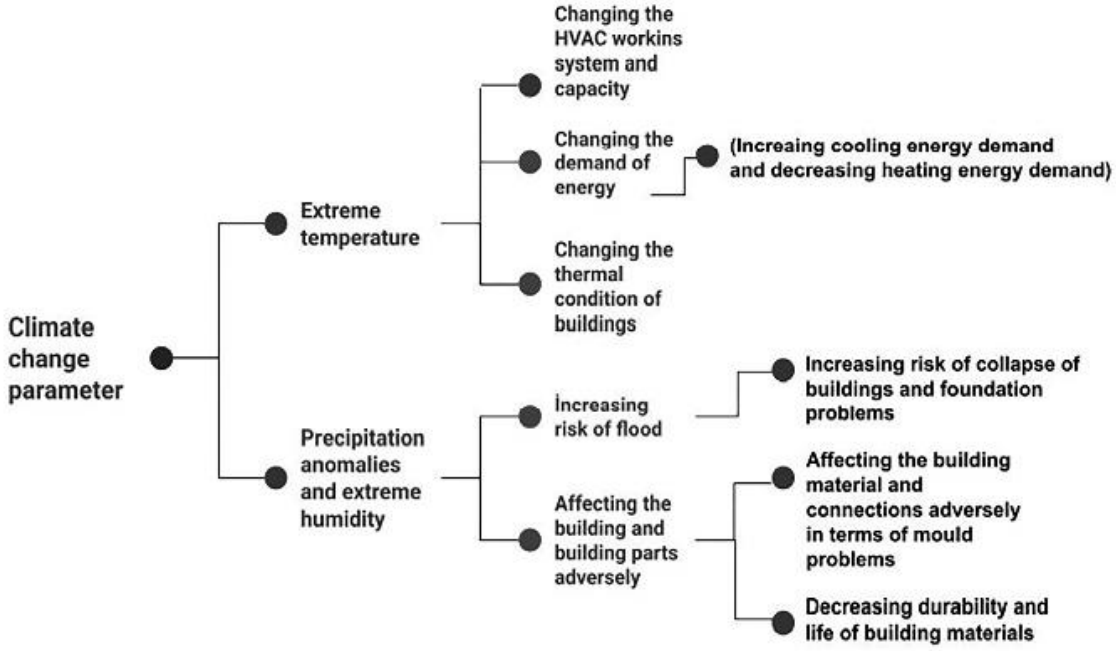



**Figure 1.** Climate change effects on buildings and building equipment [33]

It is important to understand how these impacts will affect structures/building materials to be prepared for possible changes in the future.

### 1.2. Condensation Risk and the Glaser Method

Moisture condensation is one of the main causes of undesirable effects on building envelopes in terms of materials deterioration, increasing the thermal conductivity of insulation, weakening structures, and growing mold and mildew [17]. Mold and mildew growth are consequences of moisture condensation. These fungi thrive in damp environments and can cause respiratory problems, allergies and other health concerns. They also create unpleasant smells and stains that can be difficult to remove.

There are many causes for moisture issues (accumulation) in building walls, such as using wet materials during construction, capillary rise from the ground, rainwater infiltration or melting snow penetration, water pipe leaks, persistently high humidity levels and condensation of water vapor that traverses exterior walls. In the literature, several approaches have been given to address condensation issues, as discussed by Glaser, Krischer et al., Luikov, Philip et al. and Bellia and Minichiello [34],[35],[36],[37],[38]. Although the Glaser method was first announced in 1957, condensation control in wall sections is still included in the standards of countries with this method [39]. TS 825 explains in detail how to make condensation risk calculations for a wall section using the Glaser method [39]. Also, this standard matches with ISO EN 13788 [20]. This European standard, which is also used in Turkey, includes a method with some formulas for assessing the risk of other internal surfaces' condensation problems.

In the Glaser method, first the monthly average temperature and relative humidity values for one year are obtained from a related source and after the indoor-outdoor conditions are considered constant, vapor pressures and partial vapor pressures are calculated and placed on the wall section then condensation is evaluated. According to this method, the point of condensation is when the value of vapor pressure intersects the partial vapor pressure. In addition, the material properties used in this method are constant and the effects of heavy rain and sunlight are not taken into account [40].

TS 825 explains step by step how to perform condensation analysis in a building envelope according to the Glaser method. Accordingly, the thermophysical properties of the materials that make up the building envelope must be known to conduct condensation risk analysis: thermal conductivity calculation value, water vapor diffusion resistance factor, thermal resistance and water vapor diffusion – equivalent air layer thickness [39].

For indoor and outdoor conditions, indoor temperature and relative humidity values are taken as a constant temperature and relative humidity value in the annexes of the same standard according to the type of building and are considered constant for all months within one year. For outdoor conditions, average monthly temperature and relative humidity values for each month for one year are required. These values can be used from the measurements in the studies or according to the climate zone as included in the standard or from GDM [39].

Then, the wall section's condensation status must be checked every month for one year. For this, the heat flow density of the building envelope for each month is calculated with the formulas given in [39]. After finding the temperatures of each surface with a heat flow density value, the water vapor saturation pressures and partial water vapor pressure values corresponding to these temperatures are matched or calculated with the formulas given in the standard. Finally, these values are shown on a graph for each month and, if the partial water vapor pressure values and saturated water vapor pressure values intersect, condensation is present.

### 1.3. The Strategies of Reducing the Condensation Risks on Wall Sections

Rain and humidity cause deterioration as a result of the façade's interaction with the outside environment. Also, façade surface area, room volume and material type affect the condensation risk of a wall [41].

The likelihood of condensation is greatly influenced by inadequate interior air ventilation. Surface condensation appears because most of the current building stock has inadequate ventilation [42]. According to Liu et al. [43], ventilation systems can minimize condensation by 20%; however, it should be noted that not all regions will benefit from this finding.

In order to mitigate condensation risk in wall sections in the context of climate change, it is crucial to incorporate proper design and construction practices that account for current and future climate conditions [44]. This can include implementing moisture management strategies, such as proper ventilation and insulation techniques, to reduce the potential for warm, humid air to come into contact with the cold surfaces within the wall section [45].

The resulting moisture can promote the growth of mold and mildew, degrade building materials, and compromise the structural integrity of the wall section. Therefore, it is essential to implement effective design and construction strategies, such as proper insulation and vapor barriers, adequate ventilation systems, and regular maintenance practices to mitigate condensation risk in wall sections. In addition, regular monitoring and inspection of wall sections can help detect and address condensation issues in a timely manner, preventing further damage and maintaining the overall performance and longevity of the wall section [46]. Furthermore, considering the differences in temperature and moisture sources between the parapet wall and exterior walls enclosing the interior space of a building is essential [47]. Moreover, exploring the impact of climate adaptation strategies, such as green roofs or rainwater harvesting

systems, on condensation risk in wall sections is important [48]. Also, analyzing the role of materials with improved moisture control properties, such as hydrophobic coatings or moisture-absorbing composites, in reducing condensation risk in wall sections is essential [27]. Investigating the effectiveness of novel insulation materials and techniques in mitigating condensation risk in wall sections under changing climate conditions helps to prevent condensation risk. Thanks to developing predictive models and tools that incorporate climate data, building characteristics, and occupant behavior to assess and predict condensation risk in wall sections under various climatic scenarios will help architects and engineers todesign the buildings and parts against climate change adverse effects.

In today's rapidly changing world, the significance of accurate weather forecasts cannot be overstated [49]. Accurate weather forecasts are crucial for understanding the changing climate conditions and their potential impact on condensation risk in wall sections. In summary, the increased risk of condensation in wall sections due to climate change necessitates the implementation of effective design strategies, regular maintenance practices, and proper monitoring to mitigate condensation issues and protect the integrity of wall sections.

In summary, the risk of condensation in a wall section is increased due to climate change and its associated effects, such as rising temperatures and changing precipitation patterns. As climate change continues to progress, the risk of condensation within wall sections is expected to increase. Therefore, it is essential for architects and builders to consider these factors and adapt their design and construction practices to address the increased condensation risk in wall sections in the face of climate change.

Future research trends should focus on understanding the complex interaction between changing climate conditions, building design and materials, urban planning strategies, and occupant behavior. This will help in developing effective mitigation strategies and technologies to minimize condensation risk, ensure the durability and performance of buildings, and create resilient and sustainable built environments for the future.

### 1.4. Future Research Trends

Future research could include hygrothermal simulation programs. In this way, more precise analyses can be made using hourly data. In addition, the analysis performed by the Glaser method in this study can be achieved with simulation programs, and the results can be compared.

In future research, in addition to the future climate change scenario RCP 2.6 used in this study, RCP 4.5 and R.C.P. 8 scenarios and more global climate models can be used to compare the results.

Moreover, it could be studied that investigating the potential impact of extreme weather events, such as hurricanes and heavy rainfall, on condensation risk and developing strategies to mitigate their effects on building envelope integrity and condensation risk. Also, it could be thought that investigating the potential impact of rising sea levels on condensation risk in coastal regions, including the developing strategies to protect buildings from saltwater intrusion and its contribution to increased moisture levels and condensation risk in wall sections.

With simulation programs that perform hygrothermal analysis using hourly data that consider dynamic factors such as real-time weather changes and changing climatic conditions, more comprehensive analyses can be performed using wall sections of different building types.

Ventilated facades can be included in the analyses, and in addition to wall layers, wall joints can be examined under different future scenarios in terms of humidity and temperature with advanced simulation programs.

In addition, mitigation strategies that can be applied for moisture control in a wall section can be an element of investigation. In this context, it should be done investigating the role of ventilation strategies in reducing condensation risk and maintaining indoor air quality. Also, it should be studied to explore the impact of building orientation, shading, and insulation on condensation risk in different climate zones. With analyzing the effectiveness of moisture control measures, such as vapor barriers and air sealing, in minimizing condensation risk in wall sections is important.

Kinetic and controllable smart facades and their layers can be studied under varying climatic conditions. In this context, it should be studied that evaluating the potential benefits and drawbacks of incorporating smart technologies, such as sensors and actuators, to actively monitor and control moisture levels in wall sections under changing climate conditions.

The damages caused by moisture problems in wall sections under changing climatic conditions can be considered economically. For example, it is thought that assessing the economic implications of condensation risk and potential cost-effective strategies for mitigating it in different building types.

One of the influential factors in the control of heat and humidity in buildings can be the subject of human behavior. So, examining the influence of occupant behavior on condensation risk and developing strategies to promote behavior changes that reduce moisture production and increase ventilation is essential.

## 2. Materials and Methods

As seen in **Figure 2**, for a wall section, temperature and relative humidity data from three global climate change models (HadGEM, GFDL and MPI) are obtained from GDM for 2081. These data also include data from the RCP 8.5 scenario and 2015, which was chosen as the reference year for the same location. The Glaser in-section condensation control method is then described, condensation analysis is conducted on a sample building wall section for the reference year (2015) and the future projection (2081), and the condensation risks in the reference year and future period are compared.

### 2.1. Projections and Comparisions of the GCM Models

First, monthly average temperature and relative humidity data for Zonguldak province for the historical period of

2015 and future period of 2081 were obtained from GDM. Station numbers, GCMs and location information of the obtained data are given in **Table 1**.

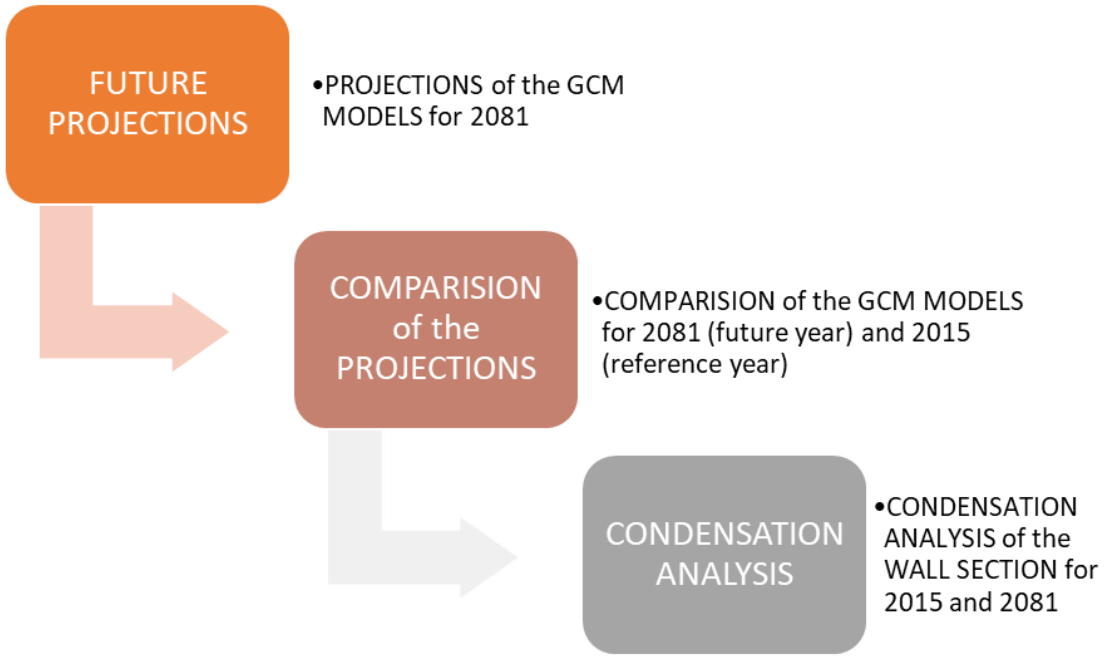



**Figure 2.** This study's method steps (created by authors)

**Table 1.** Station grid numbers and names from which climate data are obtained (GDM)

| **Information about the Data Obtained** | **Historical Year:**<br>**2015** | **Future Year:**<br>**2081** |
|---|---|---|
| **Location Description** | Zonguldak<br>Latitude: 41.4564, Longitude: 31.7986 41 ° 27′ 23″ north, 31 °47′ 55″ east | Zonguldak<br>Latitude: 41.4564, Longitude: 31.7986 41 ° 27′ 23″ north, 31 °47′ 55″ east |
| **GCMs** | - | GFDL, MPI, HadGEM |
| **Station Grid Numbers and Names** | Devrek/17613, Çaycuma Havalimanı/17023, Alaplı/18265, Gökçebey/18267, Acısu Tepesi Radar Sahası/17018, Güney Mendirek Feneri/17453, 17022, Ereğli/17611 | 3329 |

According to **Figure 3.c** (GFDL climate change model), the lowest temperature is **3.6ºC in January** and the highest is **22ºC in July**. While the highest value in terms of relative humidity is **87.5% in December**, the lowest is **45.4% in June**. According to **Figure 3.b.** (HadGEM climate change model), the lowest temperature is **5.1ºC in December** and the highest is **30.8ºC in July**. While the highest value in terms of relative humidity is **87.2% in December**, the lowest is **33.2% in July**. According to **Figure 3.a.** (MPI climate change model), the lowest temperature is **4ºC in January** and the highest is **26.1ºC in June**. While the highest value in terms of relative humidity is **88.9% in January**, the lowest is **32.4% in June**. In addition, according to **Figure 4**, according to the annual average temperature and relative humidity values of the stations located in different grids of Zonguldak province in 2015, the lowest temperature is **4.2ºC in January** and the highest is **23.7ºC in August**. Among the relative humidity values, the lowest average is **66% in April** and the highest is **84% in October**.

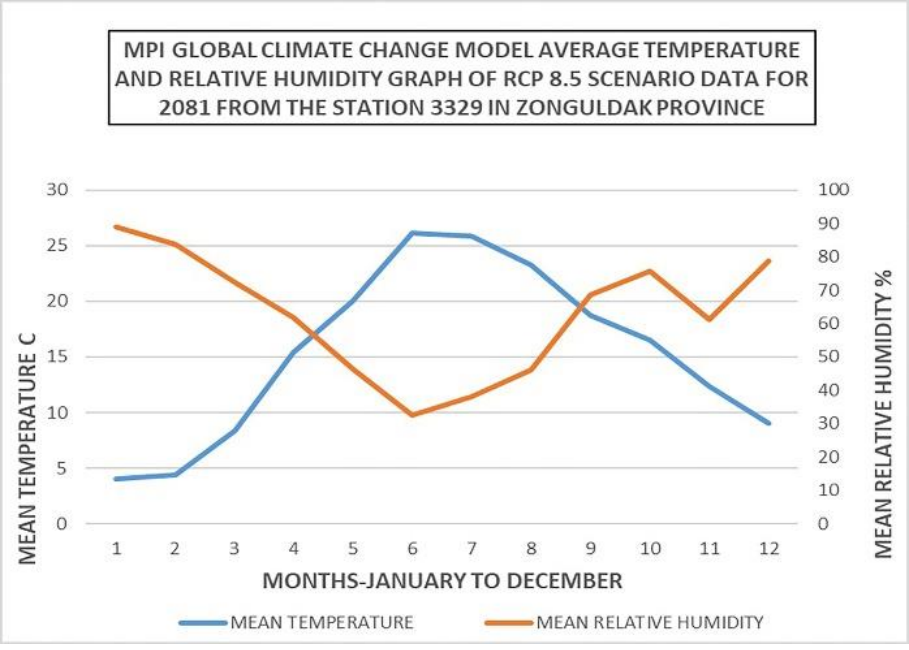



**Figure 3.** a. Average temperature and relative humidity values from station 3329 according to GFDL GCM outputs and RCP 8.5 scenario for 2081

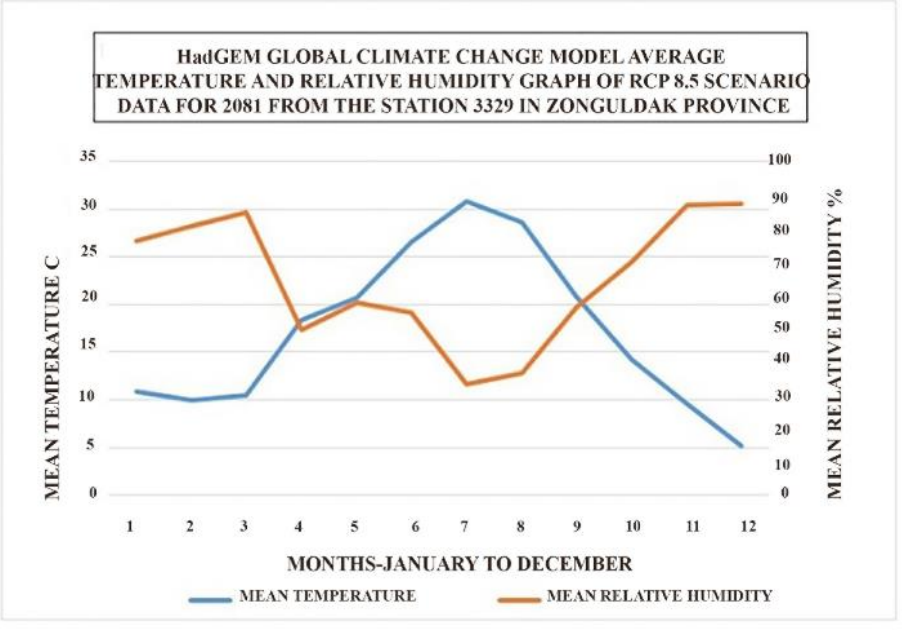



**Figure 3.** b. Average temperature and relative humidity values from station 3329 according to HadGEM GCM outputs and RCP 8.5 scenario for 2081

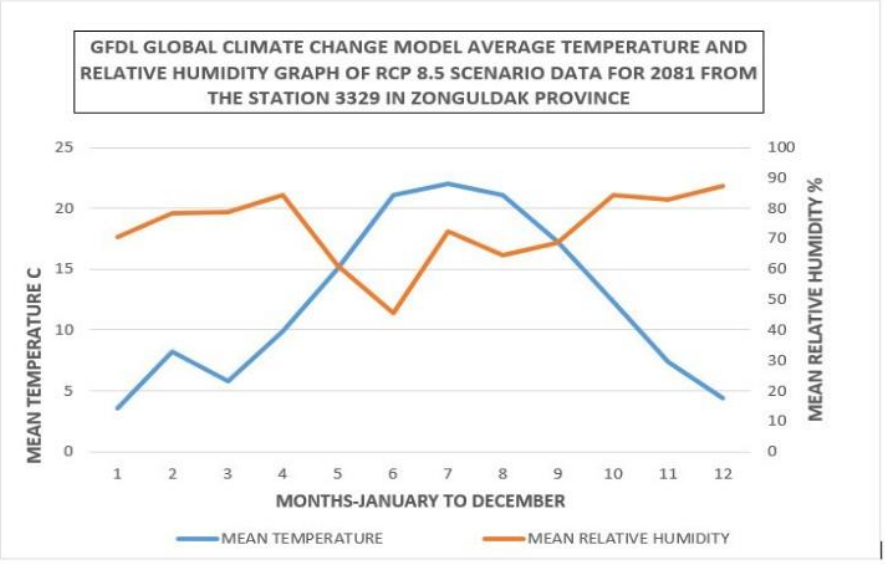



**Figure 3.** c. Average temperature and relative humidity values from station 3329 according to MPI GCM outputs and RCP 8.5 scenario for 2081

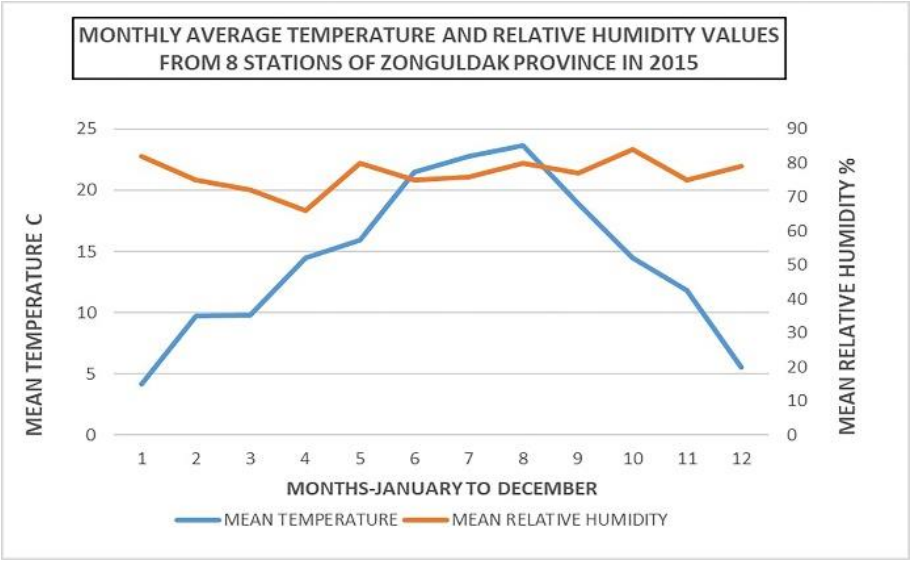



**Figure 4.** Average temperature and relative humidity values from the eight stations of Zonguldak province for 2015

### 2.2. Wall Section Condensation Risk Analysis Based on the Future Projections and Reference Year

Based on these GCM model outputs and 2015 data for Zonguldak, a basic traditional wall section condensation risk analysis was performed using the Glaser method.

First, the thermophysical properties **(Table 2)** of a wall section **(Figure 5)** prepared for condensation risk analysis using the Glaser method were obtained from TS 825 [39].

Then, using the thermophysical values of the layers given in Table 2, calculations such as the U-value and total thickness of the air layer were made to calculate the heat flow densities required for the next stage according to the same standard. For the final condensation check, the necessary calculations were made using the values found in the previous stages and the saturated and partial water vapor pressures were calculated for each month and shown in Table 3. These layer properties are also used for all analyses.

For 2015, the water vapor saturation pressure and water vapor partial pressure calculated for each month are presented in **Table 3.**

Then, the surface and ambient temperature distributions calculated from the monthly mean temperature and relative humidity values of station 3329 in the Zonguldak grids of the MPI, GFDL and HadGEM GCMs for 2081 and the saturated water vapor and partial water vapor values calculated from these values are shown in Tables **4, 5 and 6.**

**Table 2.** Thermophysical properties of building components [39]

| **Column** | **1** | **2** | **3** | **4** | **5** | **6** | **7** | **8** |
|---|---|---|---|---|---|---|---|---|
| Num. | Layer | Layer Thickness<br>d | Coefficient of water vapor diffusion resistance<br>⌈ | Diffusion equivalent air layer thickness<br>Sd = (μ.d) | Diffusion equivalent air layer thickness (cumulative)<br>$S_{dT}$= | Thermal conductivity value<br>⌊h | Resistance to heat transfer, heat resistance of material<br>R | Resistance to heat transfer, heat resistance of material<br>$R_T$ |
| - | - | m | - | m | m | W/(m.K) | $m^2$.K/W | $m^2$.K/W |
| 1. | Inner surface thermal conductivity resistance | | | | | | **0.25** | **0.25** |
| 2. | Interior plaster | **0.02** | **15** | **0.3** | **0.3** | **1** | **0.02** | **0.27** |
| 3. | Aerated concrete wall | **0.25** | **7.9** | **1.975** | **2.275** | **0.13** | **1.923** | **2.193** |
| 4. | Cement based exterior plaster | **0.03** | **25** | **0.75** | **3.025** | **1.2** | **0.025** | **2.218** |
| 5. | Rock wool insulation | **0.04** | **1** | **0.04** | **3.065** | **0.035** | **1.1428** | **3.360** |
| 6. | Mineral based exterior plaster | **0.02** | **25** | **0.5** | **3.565** | **0.8** | **0.025** | **3.385** |
| 7. | Outdoor surface thermal conductivity resistance | - | - | - | - | - | **0.04** | **3.425** |
| **$S_{dT}$ = 3.565** | | | | | | | | **1/U= 3.425** |

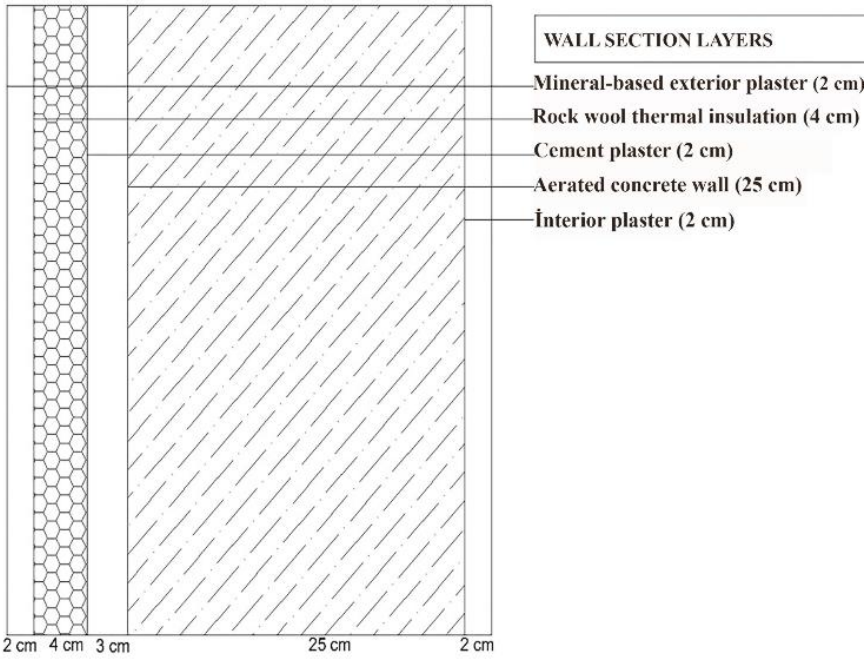



**Figure 5.** Wall section and layers

**Table 3.** Water vapor saturation and partial pressure values according to 2015 GDM data for Zonguldak province

| MONTHS | $\theta_{outdoor\ Env.}$ | $\theta_{yd} = \theta_d + Re.q$ | $\theta_4$ | $\theta_3$ | $\theta_2$ | $\theta_1$ | $\theta_{yi} = \theta_i - R_{i.q}$ | $\theta_{indoor\ Env.}$ | |
|---|---|---|---|---|---|---|---|---|---|
| JANUARY | 834 | 836 | 856 | 1309 | 1319 | 2569 | 2584 | 2805 | SATURATED VAPOR PRESSURE |
| | | | | | | | | 1683 | PARTIAL VAPOR PRESSURE |
| FEBRUARY | 1202 | 1214 | 1234 | 1647 | 1657 | 2634 | 2647 | 2805 | SATURATED VAPOR PRESSURE |
| | 901.5 | | | | | | | 1683 | PARTIAL VAPOR PRESSURE |
| MARCH | 1209 | 1222 | 1245 | 1656 | 1666 | 2636 | 2649 | 2805 | SATURATED VAPOR PRESSURE |
| | 870 | | | | | | | 1683 | PARTIAL VAPOR PRESSURE |
| APRIL | 1649 | 1659 | 1677 | 2004 | 2014 | 2695 | 2703 | 2805 | SATURATED VAPOR PRESSURE |
| | 1088 | | | | | | | 1683 | PARTIAL VAPOR PRESSURE |
| MAY | 1804 | 1813 | 1828 | 2120 | 2126 | 2711 | 2719 | 2805 | SATURATED VAPOR PRESSURE |
| | 1443 | | | | | | | 683 | PARTIAL VAPOR PRESSURE |
| JUNE | 2553 | 2556 | 2551 | 2631 | 2634 | 2771 | 2788 | 2805 | SATURATED VAPOR PRESSURE |
| | 1914 | | | | | | | 1683 | PARTIAL VAPOR PRESSURE |
| JULY | 2774 | 2771 | 2774 | 2785 | 2785 | 2802 | 2802 | 2805 | SATURATED VAPOR PRESSURE |
| | 2108 | | | | | | | 1683 | PARTIAL VAPOR PRESSURE |
| AUGUST | 2928 | 2925 | 2928 | 2887 | 2887 | 2822 | 2813 | 2805 | SATURATED VAPOR PRESSURE |
| | 2342 | | | | | | | 1683 | PARTIAL VAPOR PRESSURE |
| SEPTEMBER | 2173 | 2186 | 2202 | 2395 | 2397 | 2755 | 2758 | 2805 | SATURATED VAPOR PRESSURE |
| | 1673 | | | | | | | 1683 | PARTIAL VAPOR PRESSURE |
| OCTOBER | 1649 | 1659 | 1677 | 2004 | 2014 | 2695 | 2703 | 2805 | SATURATED VAPOR PRESSURE |
| | 1385 | | | | | | | 1683 | PARTIAL VAPOR PRESSURE |
| NOVEMBER | 1383 | 1393 | 1414 | 1795 | 1806 | 2660 | 2671 | 2805 | SATURATED VAPOR PRESSURE |
| | 1037 | | | | | | | 1683 | PARTIAL VAPOR PRESSURE |
| DECEMBER | 907 | 918 | 940 | 1387 | 1398 | 2584 | 2600 | 2805 | SATURATED VAPOR PRESSURE |
| | 716 | | | | | | | 1683 | PARTIAL VAPOR PRESSURE |

**Table 4.** Surface and ambient temperature distribution and corresponding saturated water vapor and partial water vapor values at station 3329 in the Zonguldak grids of the MPI GCM according to the monthly average temperature and relative humidity values for 2081

| | $q = U.(\theta_i - \theta_e)$ | $\theta$ *outdoor Env.* | $\theta_{yd} = \theta_d + R_e.q$ | $\theta_4$ | $\theta_3$ | $\theta_2$ | $\theta_1$ | $\theta_{yi} = \theta_i - R_i.q$ | $\theta$ *indoor Env.* |
|---|---|---|---|---|---|---|---|---|---|
| | | | | | | | | | |
| **January** | 5.529 | *4* | *4.22* | *4.40* | *10.72* | *10.86* | *21.50* | *21.61* | *23* |
| ***Saturated Water Vapor Pressure*** | | 812 | 825 | 836 | 1287 | 1299 | 2563 | 2580 | 2807 |
| ***Partial Water Vapor Pressure*** | | 722 | | | | | | | 1684 |
| **February** | 5.412 | *4.4* | *4.61* | *4.79* | *10.98* | *11.12* | *21.53* | *21.64* | *23* |
| ***Saturated Water Vapor Pressure*** | | 836 | 848 | 859 | 1310 | 1322 | 2567 | 2584 | 2807 |
| ***Partial Water Vapor Pressure*** | | 700 | | | | | | | 1684 |
| **March** | 4.248 | *8.4* | *8.56* | *5.51* | *10.37* | *10.48* | *18.66* | *18.75* | *23* |
| ***Saturated Water Vapor Pressure*** | | 1101 | 1113 | 898 | 1258 | 1267 | 2150 | 2164 | 2807 |
| ***Partial Water Vapor Pressure*** | | 794 | | | | | | | 1684 |
| **April** | 2.211 | *15.4* | *15.48* | *15.54* | *18.07* | *18.13* | *22.39* | *22.44* | *23* |
| ***Saturated Water Vapor Pressure*** | | 1748 | 1757 | 1764 | 2071 | 2079 | 2705 | 2714 | 2807 |
| ***Partial Water Vapor Pressure*** | | 1082 | | | | | | | 1684 |
| **May** | 0.873 | *20* | *20.03* | *20.05* | *21.05* | *21.08* | *22.76* | *22.78* | *23* |
| ***Saturated Water Vapor Pressure*** | | 2336 | 2341 | 2344 | 2493 | 2497 | 2767 | 2770 | 2807 |
| ***Partial Water Vapor Pressure*** | | 1086 | | | | | | | 1684 |
| **June** | -0.902 | *26.01* | *26.08* | *26.01* | *24.98* | *24.96* | *23.23* | *23.22* | *23* |
| ***Saturated Water Vapor Pressure*** | | 3379 | 3375 | 3361 | 3162 | 3158 | 2847 | 2845 | 2807 |
| ***Partial Water Vapor Pressure*** | | 1094 | | | | | | | 1684 |
| **July** | -0.843 | *25.9* | *25.86* | *25.82* | *24.86* | *24.84* | *23.22* | *23.21* | *23* |
| ***Saturated Water Vapor Pressure*** | | 3339 | 3331 | 3323 | 3139 | 3135 | 2845 | 2843 | 2807 |
| ***Partial Water Vapor Pressure*** | | 1268 | | | | | | | 1684 |
| **August** | -0.087 | *23.3* | *23.29* | *23.27* | *23.18* | *23.18* | *23.02* | *23.02* | *23* |
| ***Saturated Water Vapor Pressure*** | | 2859 | 2857 | 2853 | 2838 | 2838 | 2811 | 2811 | 2807 |
| ***Partial Water Vapor Pressure*** | | 1315 | | | | | | | 1684 |
| **September** | 1.251 | *18.7* | *18.75* | *18.77* | *20.20* | *20.24* | *22.65* | *22.68* | *23* |
| ***Saturated Water Vapor Pressure*** | | 2155 | 2162 | 2164 | 2366 | 2371 | 2748 | 2753 | 2807 |
| ***Partial Water Vapor Pressure*** | | 1480 | | | | | | | 1684 |
| **October** | 1.891 | *16.5* | *16.57* | *16.21* | *18.38* | *18.43* | *22.48* | *22.52* | *23* |
| ***Saturated Water Vapor Pressure*** | | 1876 | 1884 | 1841 | 2112 | 2119 | 2720 | 2727 | 2807 |
| ***Partial Water Vapor Pressure*** | | 1422 | | | | | | | 1684 |
| **November** | 3.084 | *12.4* | *12.52* | *12.60* | *16.13* | *16.21* | *22.15* | *22.22* | *23* |
| ***Saturated Water Vapor Pressure*** | | 1439 | 1450 | 1458 | 1832 | 1841 | 2666 | 2678 | 2807 |
| ***Partial Water Vapor Pressure*** | | 881 | | | | | | | 1684 |
| **December** | 4.074 | *9* | *9.16* | *9.28* | *13.94* | *14.05* | *21.89* | *21.98* | *23* |
| ***Saturated Water Vapor Pressure*** | | 1147 | 1159 | 1169 | 1594 | 1602 | 2624 | 2639 | 2807 |
| ***Partial Water Vapor Pressure*** | | 903 | | | | | | | 1684 |

**Table 5.** Surface and ambient temperature distribution and corresponding saturated water vapor and partial water vapor values at station 3329 in the Zonguldak grids of the GFDL GCM according to the monthly average temperature and relative humidity values for 2081

| | $q = U.(\theta_i - \theta_e)$ | $\theta$ *outdoor Env.* | $\theta_{yd} = \theta_d + R_e.q$ | $\theta_4$ | $\theta_3$ | $\theta_2$ | $\theta_1$ | $\theta_{yi} = \theta_i - R_i.q$ | $\theta$ *indoor Env.* |
|---|---|---|---|---|---|---|---|---|---|
| **January** | 5.645 | *3.6* | *3.82* | *4* | *10.45* | *10.6* | *21.46* | *21.58* | *23* |
| ***Saturated Water Vapor Pressure*** | | 790 | 802 | 812 | 1264 | 1277 | 2556 | 2577 | 2807 |
| ***Partial Water Vapor Pressure*** | | 558 | | | | | | | 1684 |
| **February** | 4.306 | *8.2* | *8.37* | *8.5* | *13.43* | *13.54* | *21.83* | *21.92* | *23* |
| ***Saturated Water Vapor Pressure*** | | 1086 | 1099 | 1109 | 1539 | 1550 | 2615 | 2629 | 2807 |
| ***Partial Water Vapor Pressure*** | | 849 | | | | | | | 1684 |
| **March** | 5.00 | *5.8* | *6* | *6.15* | *11.87* | *12* | *21.63* | *21.74* | *23* |
| ***Saturated Water Vapor Pressure*** | | 921 | 934 | 944 | 1389 | 1401 | 2583 | 2600 | 2807 |
| ***Partial Water Vapor Pressure*** | | 724 | | | | | | | 1684 |
| **April** | 3.812 | *9.9* | *10.15* | *10.26* | *14.59* | *14.69* | *21.97* | *22.05* | *23* |
| ***Saturated Water Vapor Pressure*** | | 1227 | 1239 | 1248 | 1659 | 1670 | 2637 | 2650 | 2807 |
| ***Partial Water Vapor Pressure*** | | 1036 | | | | | | | 1684 |
| **May** | 2.328 | *15* | *15.09* | *15.15* | *17.82* | *17.88* | *22.36* | *22.41* | *23* |
| ***Saturated Water Vapor Pressure*** | | 1704 | 1714 | 1720 | 2039 | 2047 | 2700 | 2709 | 2807 |
| ***Partial Water Vapor Pressure*** | | 1042 | | | | | | | 1684 |
| **June** | 0.552 | *21.1* | *21.12* | *21.11* | *21.75* | *21.77* | *22.84* | *22.86* | *23* |
| ***Saturated Water Vapor Pressure*** | | 2500 | 2503 | 2502 | 2602 | 2605 | 2780 | 2784 | 2807 |
| ***Partial Water Vapor Pressure*** | | 1135 | | | | | | | 1684 |
| **July** | 0.291 | *22* | *22.01* | *22* | *22.34* | *22.35* | *22.91* | *22.92* | *23* |
| ***Saturated Water Vapor Pressure*** | | 2642 | 2644 | 2642 | 2697 | 2699 | 2792 | 2794 | 2807 |
| ***Partial Water Vapor Pressure*** | | 1910 | | | | | | | 1684 |
| **August** | 0.552 | *21.1* | *21.12* | *21.11* | *21.75* | *21.77* | *22.84* | *22.86* | *23* |
| ***Saturated Water Vapor Pressure*** | | 2500 | 2503 | 2502 | 2602 | 2605 | 2780 | 2784 | 2807 |
| ***Partial Water Vapor Pressure*** | | 1135 | | | | | | | 1684 |
| **September** | 1.658 | *17.3* | *17.36* | *17.4* | *19.3* | *19.35* | *22.54* | *22.58* | *23* |
| ***Saturated Water Vapor Pressure*** | | 1973 | 1981 | 1986 | 2237 | 2244 | 2730 | 2737 | 2807 |
| ***Partial Water Vapor Pressure*** | | 1357 | | | | | | | 1684 |
| **October** | 3.113 | *12.3* | *12.42* | *12.52* | *16.08* | *16.16* | *22.15* | *22.22* | *23* |
| ***Saturated Water Vapor Pressure*** | | 1429 | 1441 | 1450 | 1826 | 1835 | 2666 | 2678 | 2807 |
| ***Partial Water Vapor Pressure*** | | 1206 | | | | | | | 1684 |
| **November** | 4.539 | *7.4* | *7.58* | *7.72* | *12.91* | *13.03* | *21.76* | *21.86* | *23* |
| ***Saturated Water Vapor Pressure*** | | 1029 | 1041 | 1051 | 1488 | 1499 | 2604 | 2619 | 2807 |
| ***Partial Water Vapor Pressure*** | | 853 | | | | | | | 1684 |
| **December** | 5.412 | *4.4* | *4.61* | *4.79* | *10.98* | *11.12* | *21.53* | *21.64* | *23* |
| ***Saturated Water Vapor Pressure*** | | 836 | 848 | 859 | 1310 | 1322 | 2567 | 2584 | 2807 |
| ***Partial Water Vapor Pressure*** | | 732 | | | | | | | 1684 |

**Table 6.** Surface and ambient temperature distribution and corresponding saturated water vapor and partial water vapor values at station 3329 in the Zonguldak grids of the HadGEM GCM according to the monthly average temperature and relative humidity values for 2081

| | $q = U.(\theta_i - \theta_e)$ | $\theta$ *outdoor Env.* | $\theta_{yd} = \theta_d + R_e.q$ | $\theta_4$ | $\theta_3$ | $\theta_2$ | $\theta_1$ | $\theta_{yi} = \theta_i - R_i.q$ | $\theta$ *indoor Env.* |
|---|---|---|---|---|---|---|---|---|---|
| **January** | 3.550 | *10.8* | *10.94* | *11.14* | *15.17* | *15.26* | *22.04* | *22.11* | *23* |
| ***Saturated Water Vapor Pressure*** | | 1294 | 1306 | 1324 | 1723 | 1733 | 2648 | 2660 | 2807 |
| ***Partial Water Vapor Pressure*** | | 983 | | | | | | | 1684 |
| **February** | 3.812 | *9.9* | *10.15* | *10.26* | *14.59* | *14.69* | *21.97* | *22.05* | *23* |
| ***Saturated Water Vapor Pressure*** | | 1219 | 1239 | 1248 | 1659 | 1670 | 2637 | 2650 | 2807 |
| ***Partial Water Vapor Pressure*** | | 980 | | | | | | | 1684 |
| **March** | 3.637 | *10.5* | *10.64* | *10.75* | *14.91* | *15.01* | *22.01* | *22.09* | *23* |
| ***Saturated Water Vapor Pressure*** | | 1269 | 1280 | 1290 | 1694 | 1705 | 2644 | 2656 | 2807 |
| ***Partial Water Vapor Pressure*** | | 1073 | | | | | | | 1684 |
| **April** | 1.338 | *18.4* | *18.45* | *18.48* | *20.01* | *20.05* | *22.63* | *22.66* | *23* |
| ***Saturated Water Vapor Pressure*** | | 2115 | 2121 | 2125 | 2338 | 2344 | 2745 | 2750 | 2807 |
| ***Partial Water Vapor Pressure*** | | 1046 | | | | | | | 1684 |
| **May** | 0.669 | *20.7* | *20.72* | *20.73* | *21.50* | *21.52* | *22.81* | *22.83* | *23* |
| ***Saturated Water Vapor Pressure*** | | 2440 | 2443 | 2444 | 2562 | 2566 | 2775 | 2779 | 2807 |
| ***Partial Water Vapor Pressure*** | | 1403 | | | | | | | 1684 |
| **June** | -1.0185 | *26.5* | *26.45* | *26.40* | *25.24* | *25.22* | *23.27* | *23.25* | *23* |
| ***Saturated Water Vapor Pressure*** | | 3460 | 3449 | 3439 | 3211 | 3207 | 2853 | 2850 | 2807 |
| ***Partial Water Vapor Pressure*** | | 1889 | | | | | | | 1684 |
| **July** | -2.269 | *30.8* | *30.7* | *30.60* | *28.01* | *27.96* | *23.60* | *23.56* | *23* |
| ***Saturated Water Vapor Pressure*** | | 4438 | 4413 | 4388 | 3779 | 3768 | 2911 | 2904 | 2807 |
| ***Partial Water Vapor Pressure*** | | 1473 | | | | | | | 1684 |
| **August** | -1.629 | *28.6* | *28.53* | *28.46* | *26.60* | *26.56* | *23.43* | *23.40* | *23* |
| ***Saturated Water Vapor Pressure*** | | 3911 | 3895 | 3880 | 3480 | 3472 | 2881 | 2876 | 2807 |
| ***Partial Water Vapor Pressure*** | | 1427 | | | | | | | 1684 |
| **September** | 0.640 | *20.8* | *20.82* | *20.82* | *21.56* | *21.58* | *22.82* | *22.84* | *23* |
| ***Saturated Water Vapor Pressure*** | | 2455 | 2458 | 2458 | 2572 | 2575 | 2777 | 2780 | 2807 |
| ***Partial Water Vapor Pressure*** | | 1374 | | | | | | | 1684 |
| **October** | 2.560 | *14.2* | *14.30* | *14.36* | *17.29* | *17.36* | *22.29* | *22.35* | *23* |
| ***Saturated Water Vapor Pressure*** | | 1618 | 1656 | 1635 | 1972 | 1981 | 2689 | 2699 | 2807 |
| ***Partial Water Vapor Pressure*** | | 1127 | | | | | | | 1684 |
| **November** | 3.899 | *9.6* | *9.75* | *9.88* | *14.34* | *14.44* | *21.94* | *22.02* | *23* |
| ***Saturated Water Vapor Pressure*** | | 1194 | 1206 | 1217 | 1633 | 1643 | 2632 | 2645 | 2807 |
| ***Partial Water Vapor Pressure*** | | 1037 | | | | | | | 1684 |
| **December** | 5.208 | *5.1* | *5.30* | *5.46* | *11.42* | *11.56* | *21.58* | *21.69* | *23* |
| ***Saturated Water Vapor Pressure*** | | 878 | 890 | 900 | 1349 | 1361 | 2575 | 2592 | 2807 |
| ***Partial Water Vapor Pressure*** | | 765 | | | | | | | 1684 |

Vapor diffusion plots are then drawn for all months for reference year and 2081. For 2015, the saturated vapor and partial vapor pressure values never intersected, but they came closest in January (Figure 6).

Figures 6, 7 and 8 show the diffusion plots for the wall sections. There is no risk of condensation in 2015. However, there is a risk in 2081 according to the GFDL and MPI climate models. Again, these risks are different and the mass of condensation should be calculated to specify the risk level. Incidentally, there is no risk based on the HadGEM climate model output.

First, in Figure 6, no condensation is detected according to the diffusion plots generated according to the monthly average temperature and relative humidity values for Zonguldak province in 2015, according to the data obtained from GDM. Here, the data obtained from GDM (Table 1), average monthly temperature and relative humidity values for the eight stations in Zonguldak province grids are used. While the most problematic month was January 2015, no condensation is observed.

As shown in Figure 7 condensation occurred in the insulation layer for the wall section in January and March 2081. In this case, the amount of condensed and evaporated water should be calculated and how much the layers in the wall section will be damaged should be checked and whether this will exceed the amount specified in the standard. There is a risk of condensation in the insulating layer based on the GFDL model in December 2081 (Figure 8). Finally, different levels of water mass condensed in the wall layer of the year 2081 according to GFDL and MPI model outputs. Moreover, the condensation risk occurs in one month based on GFDL and two months according to the MPI model. According to the results of the climate models, it is necessary to make calculations in accordance with the standard to determine whether the condensation water masses at different levels reach the limit value.

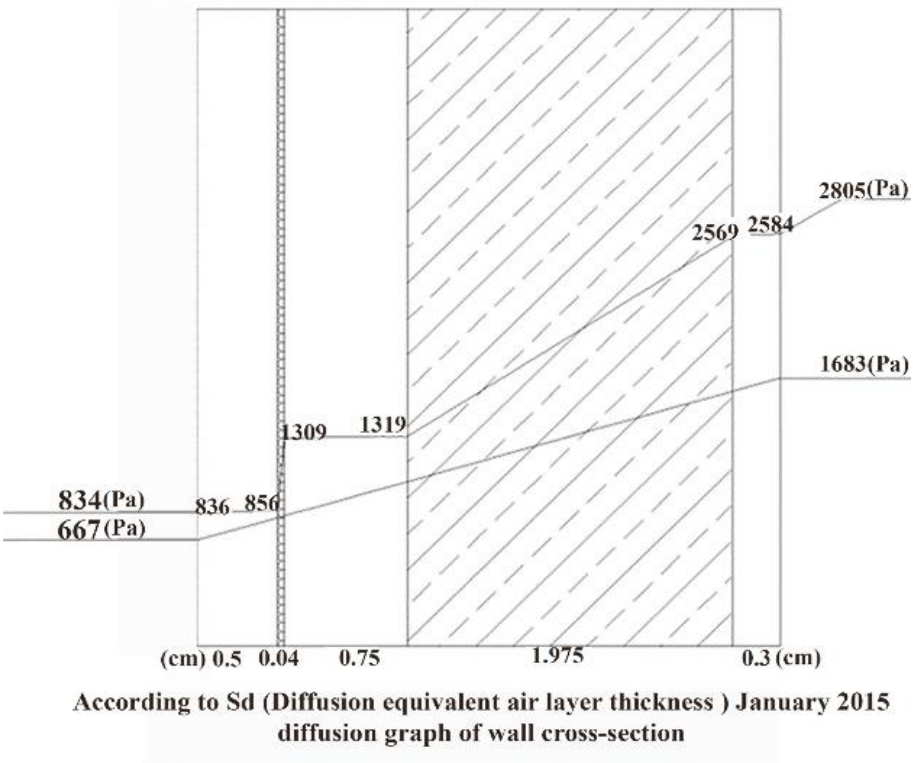
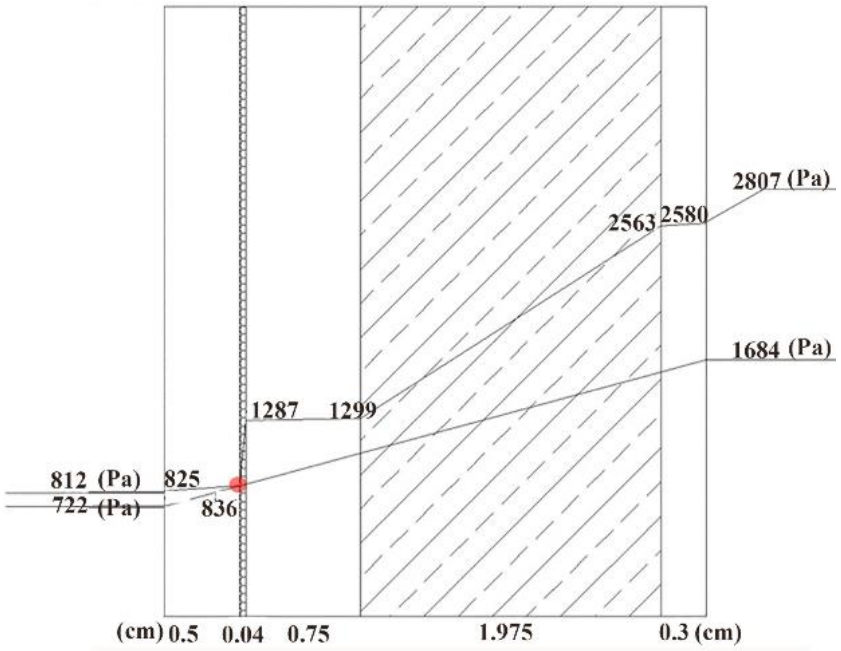
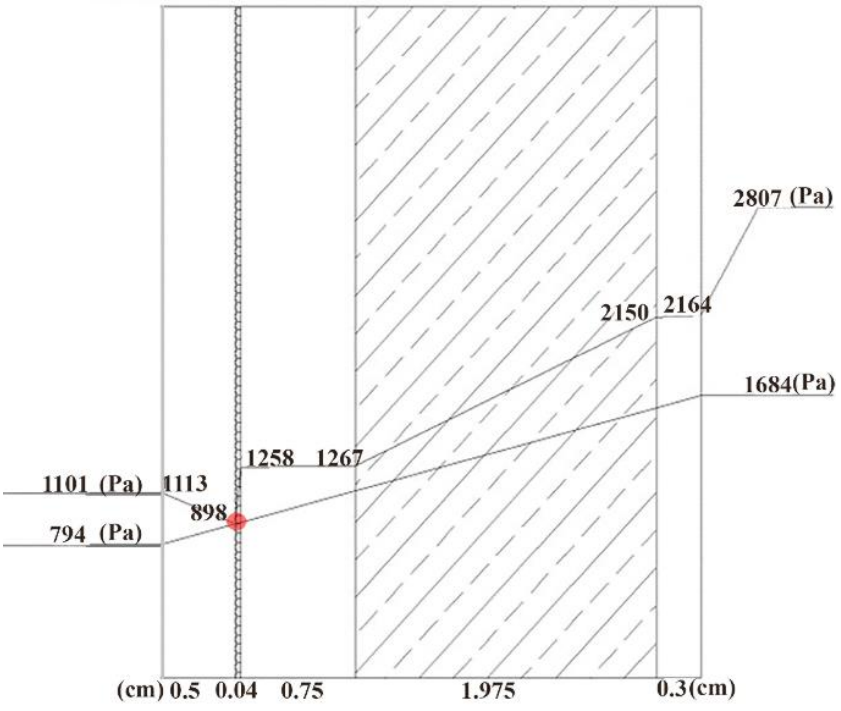



**Figure 6.** January 2015 diffusion graph of wall cross-section according to diffusion equivalent air layer thickness




Diffusion graph for January 2081 according to MPI model outputs and station 3329 data according to Sd (Diffusion equivalent air layer thickness)




Diffusion graph for March 2081 according to MPI model outputs and station 3329 data according to Sd (Diffusion equivalent air layer thickness)

**Figure 7.** January and March 2081 results of the MPI model of the diffusion diagram for the wall section according to the thickness of the diffusion equivalent air layer

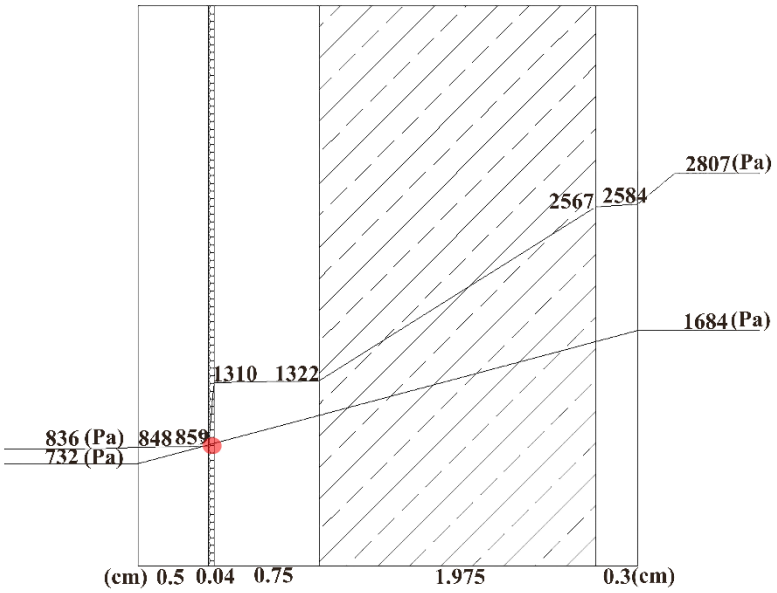



**Figure 8.** December 2081 results of the GFDL model of the diffusion diagram for the wall section according to the thickness of the diffusion equivalent air layer

## 3. Results and Discussions

The aim of this study is to first present the change in temperature and relative humidity values to show how the average temperature and relative humidity changes caused by climate change affect the condensation risk in a wall section at the building scale.

Comparing the average temperature and relative humidity values of the GCMs in 2081, shown in Table 7, with the average temperature and relative humidity values of Zonguldak province in 2015, shown in Table 8, it can be seen that the average temperatures increased according to the MPI and HadGEM predictions for 2081 compared to 2015, and decreased on average according to the GFDL model. Relative humidity, on the other hand, varied between 70-85% in 2015 and averaged around 76% throughout the year, while in 2081 it was not at a similar level throughout the year as in 2015 for all three GCMs, but fluctuated. As a result, while the GFDL model results are closest to the 2015 averages, the predictions of the other two models are higher in terms of average temperature and lower in terms of average relative humidity. Furthermore, while the coldest month in 2015 was January, the coldest month in 2081 is December in the HadGEM climate model and January in the other two models. While the hottest month in 2015 was August, the hottest month in 2081 was July for GFDL and HadGEM and June for MPI. Therefore, the hottest month shifts from August to June and July in the future. In terms of relative humidity, the highest percentage was observed in October 2015, but in December and January 2081, indicating that the months have changed. While the lowest relative humidity was observed in April 2015, these values decreased on average and changed in terms of months, becoming June and July in 2081.

**Table 7.** Future projections values as means of mean temperature and relative humidity of GCM models for 2081

| GCMs | MEAN VALUES | JANUARY | FEBRUARY | MARCH | APRIL | MAY | JUNE |
|---|---|---|---|---|---|---|---|
| MPI | MEAN T | 4 | 4.4 | 8.4 | 15.4 | 20 | 26.1 |
| | MEAN RH | 88.9 | 83.7 | 72.2 | 61.9 | 46.5 | 32.4 |
| | | JULY | AUGUST | SEPTEMBER | OCTOBER | NOVEMBER | DECEMBER |
| | MEAN T | 25.9 | 23.3 | 18.7 | 16.5 | 12.4 | 9 |
| | MEAN RH | 38 | 46 | 68.7 | 75.8 | 61.2 | 78.8 |
| | | JANUARY | FEBRUARY | MARCH | APRIL | MAY | JUNE |
| HadGEM | MEAN T | 10.8 | 9.9 | 10.5 | 18.4 | 20.7 | 26.5 |
| | MEAN RH | 76.1 | 80.4 | 84.6 | 49.5 | 57.5 | 54.6 |
| | | JULY | AUGUST | SEPTEMBER | OCTOBER | NOVEMBER | DECEMBER |
| | MEAN T | 30.8 | 28.6 | 20.8 | 14.2 | 9.6 | 5.1 |
| | MEAN RH | 33.2 | 36.5 | 56 | 69.7 | 86.9 | 87.2 |
| | | JANUARY | FEBRUARY | MARCH | APRIL | MAY | JUNE |
| GFDL | MEAN T | 3.6 | 8.2 | 5.8 | 9.9 | 15 | 21.1 |
| | MEAN RH | 70.7 | 78.2 | 78.6 | 84.5 | 61.2 | 45.4 |
| | | JULY | AUGUST | SEPTEMBER | OCTOBER | NOVEMBER | DECEMBER |
| | MEAN T | 22 | 21.1 | 17.3 | 12.3 | 7.4 | 4.4 |
| | MEAN RH | 72.3 | 64.6 | 68.8 | 84.4 | 82.9 | 87.5 |

**Table 8.** Average temperature and relative humidity for 2015

| MEAN VALUES | JANUARY | FEBRUARY | MARCH | APRIL | MAY | JUNE |
|---|---|---|---|---|---|---|
| MEAN T | 4.2 | 9.7 | 9.8 | 14.5 | 15.9 | 21.45 |
| MEAN RH | 82 | 75 | 72 | 66 | 80 | 75 |
| | JULY | AUGUST | SEPTEMBER | OCTOBER | NOVEMBER | DECEMBER |
| MEAN T | 22.8 | 23.7 | 18.9 | 14.5 | 11.8 | 5.57 |
| MEAN RH | 76 | 80 | 77 | 84 | 75 | 79 |

In addition, although the values predicted by the GFDL model for 2081 are closest to the values of 2015, it is seen that there is a risk of condensation in the wall section in 2081 as seen in Figure 8. Condensation was also observed in the wall section according to the MPI model outputs. Although the amount of condensation occurring according to this model is higher than the amount obtained according to the GFDL model, it is necessary to calculate the amount of condensation mentioned in TS 825 [39] (Figure 9) to check whether they are at the limit value according to the standard and understand which model has more risk. Accordingly, the calculations made for the MPI model follow.

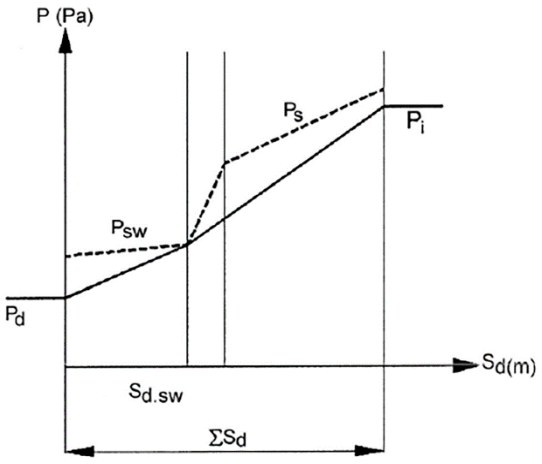



**Figure 9.** Water vapor diffusion in the presence of condensation at an interface plane within the wall section [39]

According to **Figure 9**, the calculation of the mass of condensed water for January 2081 for the MPI model (**Figure 7**) is as follows:

$$g=\delta_o\ x(P_i-P_{sw}/S_{dT}-S_{d,sw})–(P_{sw}-P_d/S_{d,sw}) \quad (1)$$

Where **g** is 'amount of water vapor per unit area' and $\delta_o$ is $2x10^{-10}$ kg/(m.s.Pa). Here $\delta_o$ is the water vapor diffusion resistance and varies slightly depending on temperature and barometric pressure. The effects of these variables are neglected in this standard and study. Here $P_i$ means 'water vapor in the air in contact with the surface of the building component in the room partial pressure' and $P_d$ shows 'water vapor in the air in contact with the outer surface of the building component partial pressure.' $P_s$ is 'saturated water vapor pressure at temperature T' and $P_{sw}$ means 'saturated water vapor pressure.' $S_d$ shows 'water vapor diffusion-equivalent air layer thickness.'

$$g=2x10^{-10}x(1684-836/3.025)-(836-722/0.54)=280.330-211.111=69.219\ x\ 2\ x\ 10^{-10}=1.38438935\ \times10^{-8}$$

Mass of total condensed water:

$$my = gxt\ (1month\ of\ time\ (86400\ x\ 30) \quad (2)$$

Here:

**my**: Amount (mass) of condensed and/or evaporated water

**g**: Amount (mass) of water condensed and/or evaporated in 1 second

**t**: 1 month time in seconds (86400 x 30)

$$my = 1.38438935\ \times10^{-8}\ x\ 86400\ x\ 30 = 0.0358833719\ kg/m^2$$

According to **Figure 9,** the calculation of the mass of condensed water for March 2081for the MPI model **(Figure 7)** is as follows:

$$g= \delta_o\ x\ (P_i-P_{sw}/S_{dT}-S_{d,sw}) –(P_{sw}-P_d/S_{d,sw})$$

$$g=2x10^{-10}x(1684-898/3.025)-(898-794/0.54)=259.834-192.592=67.2421181\ x\ 2\ x\ 10^{-10}=1.34484236\times10^{-8}$$

Mass of total condensed water:

$$my = g\ x\ t\ (1\ month\ of\ time\ (86400\ x\ 30)$$

$$my = 1.34484236\times10^{-8}\ x\ 86400\ x\ 30 = 0.03485831402\ kg/m^2$$

The total condensed water in January and March is 0.07074168592 kg/m$^2$. As a result, since there is no condensation in other months and the amount of condensed water is less than the limit value of 1 kg/m$^2$ as stated in the standard, it is within acceptable limits.

According to **Figure 9**, the calculation of the mass of condensed water for December 2081 for the GFDL model (**Figure 8**) is as follows:

$$g= \delta_o\ x\ (P_i-P_{sw}/S_{dT}-S_{d,sw}) –(P_{sw}-P_d/S_{d,sw})$$

$$g=2x10^{-10}x(1684-859/(3.565-0.54))-(859-732/0.54)=272.72-235.185=37.5420875\ x\ 2\ x\ 10^{-10}=7.5084175\ \times10^{-9}$$

Mass of total condensed water:

$$my = g\ x\ t\ (1\ month\ of\ time\ (86400\ x\ 30)$$

$$my = 7.5084175\ \times10^{-9}\ x\ 86400\ x\ 30 = 0.01946181816\ kg/m^2$$

When the results are analyzed, it is seen there was no condensation in the other months and the amount of condensed water was within acceptable limits since it was less than the limit value of 1 kg/m$^2$ as stated in the standard.

According to the condensation analyses results, when the future projections for 2015 and 2081, which were made in line with the predictions of three climatic models, are compared, the changes in average temperature and relative humidity values have led to different results in the models. However, in all cases, a general increase was observed in average values in terms of temperature and irregular peaks in terms of relative humidity compared to 2015. According to the projections for 2081, the risk of condensation in the wall section (MPI and GFDL) was observed in two climatic models, indicating that all these average changes increase the risk of condensation in the wall section.

According to the results, projections for increases in summer temperature and decreases in precipitation indicate the Mediterranean region will be one of the hotspots of climate change in the twenty-first century. In the future projections in the region where the study was conducted, it is predicted that average temperatures will increase and precipitation will decrease during the warm seasons.

In the projections made according to the results obtained in terms of building façades and façade coatings, increasing temperatures and humidity fluctuations will deteriorate the plaster and affect it in various ways. One of these effects is the deterioration of the material on plastered surfaces as a result of increased carbonation rate and depth. In addition, the effect of temperature increase can contribute to thermal expansion and subsequent deformations, resulting in more blistering and separation. Loss of adhesion problems may also be exacerbated by the expected increase in cracking in the future. This will negatively affect the service life of the material. In the plastered façades examined in the study, in addition to this negative effect on the plaster, the increasing risk of condensation over the years may also affect the insulation layer, causing the material to shrink and shorten its service life. In addition to these, detailed designs on the façades and façade elements of the buildings will gain importance to prevent deterioration. The fact that the parts of the buildings closest to the ground will be most affected by deterioration shows that skirt details in the system section will gain importance in the future. In addition, as shown in the literature studies, the use of PCMs against the effects of climate change will increase their preference for façades as they show positive results in cooling loads and thermal comfort.

# 4. Conclusions

To achieve sustainability for buildings, it is important to take climate action into account when planning the design and maintenance of façades. Climate action is unpredictable and has a cumulative effect over time. In the study, using climate change scenarios, the average

temperature and relative humidity in the future period increased compared to the reference year, and the hottest and coldest months changed. Then, investigating the effect of these changes on the thermal and moisture performance of building fa çades, the risk of condensation between fa çade layers increased in 2081 compared to 2015, and condensation was observed. This shows that climate change will have a negative impact on building fa çades.

As a result, the study presents the impact of climate change on building fa çades and building systems in a field study with a broad perspective, supported by the information obtained from the literature. The results obtained in the field study have shown the moisture-related problems that may occur in the future periods and it has been revealed that these situations will bring different results with the data from different climate models. Due to the uncertainties in climate model data, similar studies should be tested with more than one model, but it has been observed that models with more extreme values produce worse results. Although climate change projections vary according to regional conditions, designing with these projections in mind will be a necessity for architects and engineers in the future, for renovations of existing buildings and for new buildings. In addition, as regional design guidelines change from country to country, the minimum and maximum design values in standards for building envelope elements will need to be reconsidered. This is because climate change will introduce new boundary conditions that will affect design limits. Finally, it is predicted that ventilated fa çades or fa çade systems with materials produced with more adaptive and new technologies will be preferred instead of classical plastered fa çade sections in new buildings and renovations of existing building fa çades in the future.

## Acknowledgements

The authors did not receive support from any organization for the submitted work.

## REFERENCES

[1] UNCCS, “Climate action and support trends”, United Nations Climate Change Secretariat, https ://unfcc c.int/sites /defau lt/files /resou rce/Clima te_Actio n_Suppo rt_Trend s_2019.pdf. (accessed March 10, 2023).

[2] Fawzy, S., Osman, A. I., Doran, J., & Rooney, D. W., “Strategies for mitigation of climate change: a review”, Environmental Chemistry Letters, vol. 18, pp 2069-2094, 2020. DOI: 10.1007/s10311-020-01059-w.

[3] Quesada-Ganuza, L., Garmendia, L., & Gandini, A., “A framework for risk assessment”, 1 st ed, In Adapting the Built Environment for Climate Change, Woodhead Publishing, 2023, pp. 17-36.

[4] Moss, R. H., Edmonds, J. A., Hibbard, K. A., Manning, M. R., Rose, S. K., Van Vuuren, D. P., ... & Wilbanks, T. J. “The next generation of scenarios for climate change research and assessment”, Nature, vol. 463, no. 7282, pp 747-756, 2010. DOI: 10.1038/nature08823.

[5] IPCC (Intergovernmental Panel on Climate Change), “Climate change 2014: Synthesis report. Contribution of working groups I, II and III to the fifth assessment report of the Intergovernmental Panel on Climate Change”, https://archive.ipcc.ch/pdf/assessment-report/ar5/syr/SYR_AR5_FINAL_full_wcover.pdf, (accessed: 2.12.2023).

[6] Hosseini, M., Bigtashi, A., & Lee, B., “Generating future weather files under climate change scenarios to support building energy simulation–A machine learning approach”, Energy and Buildings, vol. 230, no. 110543, pp 2-5, 2021. DOI: 10.1016/j.enbuild.2020.110543.

[7] Farmer, G. T., “An Overview of Today's Climate Change Science”, in Modern Climate Change Science, 1st ed, Berlin: Springer, 2015, pp 32-34. DOI: 10.1007/978-3-319-09222-5.

[8] Dickinson, R., & Brannon, B., “Generating Future Weather Files For Resilience”, In Proceedings of the İnternational Conference on Passive and Low Energy Architecture, Los Angeles, CA, USA, Jul., 2016, pp. 11-13.

[9] Fereidani, N. A., Rodrigues, E., & Gaspar, A. R., “A Review of the Energy İmplications of Passive Building Design and Active Measures under Climate Change in the Middle East”, Journal of Cleaner Production, vol. 305, no. 127152, pp 1-13, 2021. DOI: 10.1016/j.jclepro.2021.127152.

[10] Roberts, S., “Effects of Climate Change on the Built Environment”, Energy Policy, vol. 36, no. 12, pp, 2008. 4552-4557, 2008. DOI: 10.1016/j.enpol.2008.09.012.

[11] Hrabovszky-Horváth, S., Pálvölgyi, T., Csoknyai, T., & Talamon, A., “Generalized Residential Building Typology for Urban Climate Change Mitigation and Adaptation Strategies: the case of Hungary”, Energy and Buildings, vol. 62, pp 475-485, 2013. DOI: 10.1016/j.enbuild.2013.03.011.

[12] Khourchid, Ammar M., Salah Basem Ajjur, and Sami G. Al-Ghamdi., “Building Cooling Requirements under Climate Change Scenarios: Impact, Mitigation Strategies, and Future Directions”, Buildings, vol. 12, no. 10, pp 1519, 2022. DOI: 10.3390/buildings12101519.

[13] Rahif, R., Hamdy, M., Homaei, S., Zhang, C., Holzer, P., & Attia, S., “Simulation-Based Framework to Evaluate Resistivity of Cooling Strategies in Buildings Against Overheating İmpact of Climate Change”, Building and Environment, vol. 208, no. 108599, 2022. DOI: 10.1016/j.buildenv.2021.108599.

[14] Hayles, C. S., Huddleston, M., Chinowsky, P., & Helman, J., “Summertime İmpacts of Climate Change on Dwellings in Wales, UK”, Building and Environment, vol. 219, no. 109185, pp 1-16, 2022. DOI: 10.1016/j.buildenv.2022.109185.

[15] Baborska-Narozny, M., & Grudzinska, M., “Overheating in a UK High-Rise Retrofit Apartment Block–Ranking of Measures Available to Case Study Occupants Based on Modelling”, Energy Procedia, vol. 111, pp 568-577, 2017. DOI: 10.1016/j.egypro.2017.03.219.

[16] Cascione, V., Marra, E., Zirkelbach, D., Liuzzi, S., & Stefanizzi, P., "Hygrothermal Analysis of Technical Solutions for İnsulating the Opaque Building Envelope", Energy Procedia, vol. 126, pp 203-210, 2017. DOI: 10.1016/j.egypro.2017.08.141.

[17] Biserni, C., & Imbiombato, A. N., "Numerical Analysis on Building Envelope Moisture Condensation: A Case Study using the Glaser Diagram Method, In AIP Conference Proceedings, vol. 2191, no. 1, Dec., 2019, pp 020023, AIP Publishing LLC. DOI: 10.1063/1.5138756.

[18] Taylor, J., Biddulph, P., Davies, M., Ridley, I., Mavrogianni, A., Oikonomou, E., & Lai, K. M., "Using Building Simulation to Model the Drying of Flooded Building Archetypes", Journal of Building Performance Simulation, vol. 6, no. 2, pp 119-140, 2013. DOI: 10.1080/19401493.2012.703243.

[19] Verlag B., "DIN 4108-2, Thermal Protection and Energy Economy in Buildings -Part 2: Minimum Requirements to Thermal insulation", pp 1-34, 2013. DOI: 10.31030/1929159.

[20] EN ISO 13788, "Hygrothermal Performance of Building Components and Building Elements. Internal Surface Temperature to Avoid Critical Surface Humidity and İnterstitial Condensation. Calculation Methods", pp 1-52, 2012.

[21] Yassaghi, H.; Hoque, S., "Impact Assessment in the Process of Propagating Climate Change Uncertainties into Building Energy Use", Energies 2021, vol. 14, no. 367. pp 2-27, 2021. DOI: https://doi.org/10.3390/en14020367

[22] Çağman, S., and Ünver, Ü., "Determination of Condensation and Its Effect On Insulation and Wall Envelop Layers", European Journal of Technique (EJT), vol. 13, no. 2, pp 68-73, 2023. DOI: 10.36222/ejt.1295570.

[23] Langmans, J., Piet, H., and Staf, R., "A three-dimensional steady-state heat and vapour transport model to assess the risk for interstitial condensation in building enclosures", Journal of Physics: Conference Series, vol. 2654, no. 1. IOP Publishing, 2023. DOI: 10.1088/1742-6596/2654/1/012039.

[24] Gołębiewski, M., and Pietruszka, B., "Risk of interstitial condensation in outer walls made of hemp-lime composite in Polish climatic conditions", Archives of Civil Engineering, vol. LXVII, no. 4, pp 107-121, 2021. DOI: 10.24425/ace.2021.138489.

[25] Thapa, S., "Risk of Overheating in Low-Rise Naturally Ventilated Residential Buildings of Northeast India – An Effect of Climate Change", Architectural Science Review, vol. 65, no. 1, pp 14-41, 2022. DOI: 10.1080/00038628.2021.1941748.

[26] Andric, I., A. Pina, P. Ferrao, J. Fournier, B. Lacarriere, and O. L. Corre.,"The Impact of Climate Change on Building Heat Demand in Different Climate Types", Energy and Buildings, vol. 149, pp 225–234, 2017. DOI: 10.1016/j.enbuild.2017.05.047.

[27] Lacasse, M. A., Gaur, A., & Moore, T. V., " Durability and Climate Change—Implications For Service Life Prediction And The Maintainability Of Buildings", Buildings, vol. 10, no.3, pp 53, 2020. DOI: 10.3390/buildings10030053.

[28] Blocken, B., Derome, D., & Carmeliet, J., "Rainwater Runoff from Building Facades: A Review", Building and Environment, vol. 60, pp 339-361, 2013. DOI: 10.1016/j.buildenv.2012.10.008.

[29] Hernández-Montes, E., Hdz-Gil, L., Coletti, C., Dilaria, S., Germinario, L., & Mazzoli, C., "Prediction Model for the Evolution of the Deterioration of Bricks in Heritage Buildings in Venice Caused by Climate Change", Heritage, vol. 6, no. 1, 483–491, 2023. DOI: 10.3390/heritage6010025.

[30] Barrelas, J., Silva, A., de Brito, J., & Tadeu, A., "Effects of Climate Change on Rendered Façades: Expected Degradation in a Progressively Warmer and Drier Climate—A Review Based on the Literature", Buildings, vol. 13, no. 2, pp 352, 2023. DOI: 10.3390/buildings13020352.

[31] Stagrum, A. E., Andenæs, E., Kvande, T., & Lohne, J., "Climate Change Adaptation Measures for Buildings—A Scoping Review.", Sustainability, vol. 12, no. 5, pp 1721, 2020. DOI: 10.3390/su12051721.

[32] Grøntoft, T., "Climate Change Impact on Building Surfaces and Façades", International Journal of Climate Change Strategies and Management, vol. 3, no. 4, pp 374-385, 2011. DOI: 10.1108/17568691111175669.

[33] Sarıcıoğlu, P., & Ayçam, İ., " Building Design in the Context of Climate Change And a Flood Projection for Ankara", in Adapting the Built Environment for Climate Change, 1 st ed, Woodhead Publishing, 2023, pp 327-347.

[34] Glaser, H., " Einfluss der Temperatur auf den Dampfdurchgang durch trockene Isolierwande", Kaltetechnik, 1957, pp 158– 159.

[35] Krischer,O. and Kast, W., "Die wissenschaftlichen Grundlagen der Trocknungstechnik, Dritte Auflage", Berlin: Springer- Verlag, 1978, pp 14-46.

[36] Luikov, A.V., "Systems of Differential Equations of Heat and Mass Transfer in Capillary-Porous Bodies", International Journal of Heat and Mass Transfer, vol. 18, pp 1-14, 1975. DOI: 10.1016/0017-9310(75)90002-2.

[37] Philip, J. R., & De Vries, D. D., "Moisture Movement in Porous Materials under Temperature Gradients", Eos, Transactions American Geophysical Union, vol. 38, no. 2, pp 222-232, 1957. DOI: 10.1029/TR038i002p00222.

[38] Bellia, L., & Minichiello, F., "A simple Evaluator of Building Envelope Moisture Condensation According to an European Standard", Building and Environment, vol. 38, no. 3, pp 457-468, 2003. DOI: 10.1016/S0360-1323(02)00060-4.

[39] TS 825, "Thermal insulation requirements for buildings, Institue of Turkish Standard", pp 55-70, 2013.

[40] Libralato, M., Saro, O., De Angelis, A., & Spinazzè, S., "Comparison Between Glaser Method and Heat, Air and Moisture Transient Model for Moisture Migration in Building Envelopes", in Applied Mechanics and Materials, vol. 887, Trans Tech Publications Ltd, pp. 385-392, 2019. DOI: 10.3390/en14010004.

[41] Bienvenido-Huertas, D., Rubio-Bellido, C., Sánchez-García, D., & Moyano, J., "Internal surface condensation risk in façades of Spanish social dwellings", Building Research & Information, vol. 47, no. 8, pp 928-947, 2019. DOI: 10.1080/09613218.2019.1612729.

[42] Dimitroulopoulou, C., "Ventilation in European dwellings: A review", Building and Environment, vol. 47, no. 1, pp 109–125. 2012. DOI: 10.1016/j.buildenv.2011.07.016.

[43] Liu, J., Aizawa, H., & Yoshino, H., "CFD prediction of surface condensation on walls and its experimental validation", Building and Environment, vol. 39, no. 8 SPEC. ISS., pp 905–911, 2004. DOI: 10.1016/j.buildenv.2004.01. 015.

[44] Defo, M., Lacasse, M,. "Resilience of Canadian homes and small buildings to the effects of climate change-Risk of deterioration due to condensation within wall assemblies", In E3S Web of Conferences, vol. 172, pp 2-10, EDP Sciences, 2020. DOI: 10.1051/e3sconf/202017202002.

[45] Gaur, A., Lacasse, M., and Armstrong, M., "Climate Data to Undertake Hygrothermal and Whole Building Simulations Under Projected Climate Change Influences for 11 Canadian Cities", Data, vol. 4, no. 72, pp 2-17, 2019. DOI: 10.3390/data4020072.

[46] Bastien, D., Gaasvig, M.W. "Influence of driving rain and vapour diffusion on the hygrothermal performance of a hygroscopic and permeable building envelope", Energy, vol. 164, pp 288-297, 2018. DOI: 10.1016/j.energy.2018.07.195.

[47] Hwang, I.T., Kim, G.T.,Yoo, J.H., Lee, J.S., "Improvement of the Korean Design Criteria on Wall-To-Wall Junctions to Prevent Condensation in Apartment Houses", Sustainability, vol. 11, no. 3272, pp 2-14, 2019. DOI: 10.3390/su11123272.

[48] Grynning, S., Gaarder, J. E., & Lohne, J., "Climate adaptation of school buildings through MOM–a case study", Procedia engineering, vol. 196, pp 864-871, 2017. DOI: 10.1016/j.proeng.2017.08.018.

[49] Pescaru, R. A., Dumitrescu, L., Baran, I., and Grădinaru, C.M. "Comparative Analysis of Hygrothermal Behaviour of the Exterior Walls in Transient Regime", In: IOP Conference Series: Materials Science and Engineering. IOP Publishing, pp 1-9, 2019. DOI: 10.1088/1757-899X/586/1/012011.